# BRAININFO 2023

The Eighth International Conference on Neuroscience and Cognitive Brain Information

ISBN: 978-1-68558-067-4

March 13th - 17th, 2023

Barcelona, Spain

**BRAININFO 2023 Editors**

Petre Dini, IARIA, USA/EU/Asia

Rory Lewis, University of Colorado at Colorado Springs, USA

# BRAININFO 2023

# Forward

The Eighth International Conference on Neuroscience and Cognitive Brain Information (BRAININFO 2023), held between March 13th and March 17th, 2023, continued a series of events dedicated to evaluating current achievements and identify potential ways of making use of the acquired knowledge, covering neuroscience, brain connectivity, brain intelligence paradigms, cognitive information, and specific applications.

The complexity of the human brain and its cognitive actions have been the topic of many research works for decades. Most of the findings were adapted in virtual/artificial systems with the idea of modeling them for use in human-centered medical cures, especially for neurotechnologies. Information representation, retrieval, and internal data connections still constitute a domain where solutions are either missing or in a very early stage.

We take here the opportunity to warmly thank all the members of the BRAININFO 2023 technical program committee, as well as all the reviewers. The creation of such a high-quality conference program would not have been possible without their involvement. We also kindly thank all the authors who dedicated much of their time and effort to contribute to BRAININFO 2023. We truly believe that, thanks to all these efforts, the final conference program consisted of top-quality contributions. We also thank the members of the BRAININFO 2023 organizing committee for their help in handling the logistics of this event.

We hope that BRAININFO 2023 was a successful international forum for the exchange of ideas and results between academia and industry and for the promotion of progress in the field of neuroscience and cognitive brain information.

**BRAININFO 2023 Chairs**

**BRAININFO 2023 Steering Committee**

Erwin Lemche, Institute of Psychiatry, Psychology & Neuroscience | King's College School of Medicine and Dentistry, UK
Yu-Dong (Eugene) Zhang, University of Leicester, UK
Chih Lai, University of St. Thomas Minnesota, USA
William Speier, UCLA David Geffen School of Medicine, USA
Sule Yildirim-Yayilgan, Norwegian University of Science and Technology, Norway
Ricardo Ron-Angevin, University of Málaga, Spain
Rory Lewis, University of Colorado at Colorado Springs, USA

**BRAININFO 2023 Publicity Chairs**

José Miguel Jiménez, Universitat Politecnica de Valencia, Spain
Sandra Viciano Tudela, Universitat Politecnica de Valencia, Spain

# BRAININFO 2023
## Committee

**BRAININFO 2023 Steering Committee**

Erwin Lemche, Institute of Psychiatry, Psychology & Neuroscience | King's College School of Medicine and Dentistry, UK
Yu-Dong (Eugene) Zhang, University of Leicester, UK
Chih Lai, University of St. Thomas Minnesota, USA
William Speier, UCLA David Geffen School of Medicine, USA
Sule Yildirim-Yayilgan, Norwegian University of Science and Technology, Norway
Ricardo Ron-Angevin, University of Málaga, Spain
Rory Lewis, University of Colorado at Colorado Springs, USA

**BRAININFO 2023 Publicity Chairs**

José Miguel Jiménez, Universitat Politecnica de Valencia, Spain
Sandra Viciano Tudela, Universitat Politecnica de Valencia, Spain

**BRAININFO 2023 Technical Program Committee**

Aftab Ahmad, John Jay, The City University of New York (CUNY), USA
Mariano Alcañiz Raya, Institute of Research and Innovation in Bioengineering (I3B) - Universidad Politécnica Valencia, Spain
Luis Alfredo Moctezuma, Norwegian University of Science and Technology, Norway
Saad Alqithami, Albaha University, Saudi Arabia
Gian Carlo Cardarilli, University of Rome Tor Vergata, Italy
German Castellanos-Dominguez, Universidad Nacional de Colombia, Sede Manizales, Colombia
Srijata Chakravorti, Vanderbilt University, USA
Ahana Roy Choudhury, Florida State University, USA
Shiaofen Fang, Indiana University Purdue University Indianapolis, USA
Monte Hancock, 4Digital Inc., USA
M. Shamim Kaiser, Jahangirnagar University, Bangladesh
Stamatis Karlos, University of Patras, Greece
Peter Kieseberg, St. Poelten University of Applied Sciences, Austria
Chih Lai, University of St. Thomas Minnesota, USA
Erwin Lemche, Institute of Psychiatry, Psychology & Neuroscience | King's College School of Medicine / Dentistry Department of Psychosis Studies | Section of Cognitive Neuropsychiatry, UK
Rory Lewis, University of Colorado at Colorado Springs, USA
Vasilis Megalooikonomou, University of Patras, Greece
Marta Molinas, NTNU, Norway
Rafael Morales Herrera, Universidad de Castilla-La Mancha, Spain
Ricardo Nuno Vigário, Nova School of Science and Technology, Lisbon, Portugal
Lauren Reinerman-Jones, UCF Institute for Simulation and Training, USA
Izabela Rejer, West Pomeranian University of Szczecin, Poland
Ricardo Ron Angevin, University of Málaga, Spain
Linlin Shen, Shenzhen University, China / University of Nottingham, UK / University of Macau, China

**Copyright Information**

For your reference, this is the text governing the copyright release for material published by IARIA.

The copyright release is a transfer of publication rights, which allows IARIA and its partners to drive the dissemination of the published material. This allows IARIA to give articles increased visibility via distribution, inclusion in libraries, and arrangements for submission to indexes.

I, the undersigned, declare that the article is original, and that I represent the authors of this article in the copyright release matters. If this work has been done as work-for-hire, I have obtained all necessary clearances to execute a copyright release. I hereby irrevocably transfer exclusive copyright for this material to IARIA. I give IARIA permission or reproduce the work in any media format such as, but not limited to, print, digital, or electronic. I give IARIA permission to distribute the materials without restriction to any institutions or individuals. I give IARIA permission to submit the work for inclusion in article repositories as IARIA sees fit.

I, the undersigned, declare that to the best of my knowledge, the article is does not contain libelous or otherwise unlawful contents or invading the right of privacy or infringing on a proprietary right.

Following the copyright release, any circulated version of the article must bear the copyright notice and any header and footer information that IARIA applies to the published article.

IARIA grants royalty-free permission to the authors to disseminate the work, under the above provisions, for any academic, commercial, or industrial use. IARIA grants royalty-free permission to any individuals or institutions to make the article available electronically, online, or in print.

IARIA acknowledges that rights to any algorithm, process, procedure, apparatus, or articles of manufacture remain with the authors and their employers.

I, the undersigned, understand that IARIA will not be liable, in contract, tort (including, without limitation, negligence), pre-contract or other representations (other than fraudulent misrepresentations) or otherwise in connection with the publication of my work.

Exception to the above is made for work-for-hire performed while employed by the government. In that case, copyright to the material remains with the said government. The rightful owners (authors and government entity) grant unlimited and unrestricted permission to IARIA, IARIA's contractors, and IARIA's partners to further distribute the work.

# Table of Contents

# Study on the Relationship between Postprandial Brain Function Decline and Blood Glucose Levels

Yuichi Sato, Yudai Ishikawa, Gaochao Cui, Kosuke Nagano, Fumiya Kinoshita, Hideaki Touyama

Toyama Prefectural University, Information Systems Engineering

Laboratory of Human Information

Imizushi, Japan

e-mail: u155014@st.pu-toyama.ac.jp, u255004@st.pu-toyama.ac.jp, cuigaochao@pu-toyama.ac.jp, u055016@st.pu-toyama.ac.jp, f.kinoshita@pu-toyama.ac.jp, touyama@pu-toyama.ac.jp

*Abstract*— **Post-lunch drowsiness, also known as Post-Lunch Dip (PLD), is a symptom of impaired brain function. Currently, the hypothesis that PLD is caused by an increase in postprandial blood glucose level is supported as a possible explanation for the mechanism of PLD. However, few studies have examined the relationship between postprandial brain dysfunction and blood glucose levels by measuring both simultaneously. In this study, we measured blood glucose levels and Event-Related Potential (ERP) before and after consumption of two foods with different carbohydrate contents, and examined the relationship between postprandial blood glucose fluctuations and PLD. In the high-sugar food ingestion group, two slices of bread and water were given, and the low-sugar ingestion group received low-carbohydrate bread and water. The results showed that the high-sugar food ingestion group had increased sleepiness, prolonged P300 latency, and increased early and late contingent negative variation amplitudes at 40 minutes postprandial ingestion. There were no significant differences in sleepiness, brain function, or blood glucose levels in the low-sugar ingestion group. In contrast, there was a significant increase in blood glucose levels immediately and 40 minutes after eating in the high-sugar food ingestion group resulting in brain function impairment. Therefore, it is suggested the postprandial increase in blood glucose level is related to the development of PLD. In addition, the blood glucose levels at 40 minutes after eating in the high-sugar food ingestion group were significantly lower after ERP measurement than before ERP measurement. This suggests PLD occurs during hyperglycemia and when blood glucose levels fall.**

*Keywords-Post-Lunch Dip (PLD); Event-Related Potential (ERP); P300; Contingent Negative Variation (CNV); Blood Glucose Level.*

## I. INTRODUCTION

The transient decline in brain function caused by Post Lunch Dip (PLD) [1] has been highlighted as a possible cause of human error [2][3], and it is important to establish optimal intervention methods and prevention techniques against PLD. In recent years, research hypotheses that link postprandial brain dysfunction and blood glucose fluctuations have attracted attention as a possible explanation for the pathogenesis of PLD. Although the explanation of blood glucose spikes [4] and neuropeptide inhibition [5] are representative examples, neither hypothesis has been widely recognized as a research hypothesis explaining the mechanism of PLD yet, because the evidence for each hypothesis is insufficient. One of the reasons for this is that there have been few cases in which the decline in brain function due to postprandial sleepiness has been evaluated using quantitative indices. Therefore, our research group focused on electrophysiological responses using event-related potentials, a type of electroencephalogram (EEG), as a quantitative evaluation index for PLD and conducted empirical experiments [6]. In addition to the basic rhythmic components of the EEG, such as alpha and beta waves, there is Event-Related Potential (ERP), which is induced by specific stimuli. Among ERPs, P300 and Contingent Negative Variation (CNV) are used to evaluate cognitive function and attention [7]. Our empirical experiments confirmed that simultaneous measurement of P300 and CNV is an effective objective measure of transient deterioration of brain function, fatigue, and sleep in PLD. Recently, however, Continuous Glucose Monitoring (CGM) devices have emerged that can measure blood glucose levels over time with a single puncture. CGM devices can continuously record the concentration of glucose in the interstitial fluid, which is highly correlated with blood glucose levels, using a sensor implanted in the subcutaneous tissue [8]. The CGM measures the glucose concentration in the interstitial fluid by changing the current in the enzymatic method. It has been highlighted that glucose in the interstitial fluid is slow to follow rapid fluctuations in blood glucose levels [9]. However, CGM has attracted attention as a simple and powerful tool for preventing blood glucose-related diseases because it enables monitoring of blood glucose levels over time.

Therefore, in this study, we investigated the relationship between postprandial blood glucose changes and PLD by recording blood glucose levels, P300, and CNV before and after consumption of high and low carbohydrate foods over time.

The rest of this paper is organized as follows. Section II describes the experimental protocol and the issues arising from the ERP. Section III describes the P300 and CNV analysis methods. Section IV describes the experimental

results. Section V goes into more detail regarding the relationship between postprandial brain dysfunction and blood glucose fluctuations. Section VI provides a summary of this paper.

## II. EXPERIMENTAL PROCEDURE

In this study, experiments were conducted on three groups: 1) A high-sugar food ingestion group, 2) A water-only control group, and 3) A low-sugar food ingestion group. All participants were young and healthy with no history of neurological disease. The high-sugar food ingestion group comprised 20 participants (Mean ± SD, 21.50 ± 0.86 years), the control group comprised 10 participants (Mean ± SD, 22.5 ± 0.85 years), and the low-sugar food ingestion group comprised 10 participants (Mean ± SD, 21.80 ± 1.16 years). The participants were thoroughly informed about the experiment, and their consent was obtained. This experiment was approved by the Ethics Committee of Toyama Prefectural University [R3-6].

The measurement items used in this experiment were P300, CNV, electro-oculography, the Stanford Sleepiness Scale (SSS), and reaction time from stimulus presentation to pressing the button switch. Subjects were instructed to press the button switch with their dominant hand. Blood glucose levels were measured in subjects who belonged to the high-sugar food ingestion group and the low-sugar food ingestion group. Blood glucose levels were measured in 10 subjects (Mean ± SD, 21.80 ± 1.16 years) in the high-sugar food ingestion group and in all subjects in the low-sugar food ingestion group. A FreeStyle Libre (Abbott Japan LLC), a CGM device, was used to reduce the measurement burden on subjects and to minimize measurement error due to needle puncture position. CGM records the glucose concentration in the interstitial fluid, not the blood glucose concentration. However, since the glucose concentration in the interstitial fluid has been reported to have a high correlation with the blood glucose concentration, the glucose concentration in the interstitial fluid is hereafter referred to as the blood glucose level. The sensor for measuring blood glucose was attached to the side of the upper arm opposite the dominant hand of each subject.

A g.USBamp (g.tec medical engineering GmbH, Austria) was used to measure biological signals. The sampling frequency of the measurement device was 512 Hz, and a low-pass filter of 0.01 Hz, a high-pass filter of 30 Hz, and a notch filter of 60 Hz were applied for noise reduction. Based on the extended 10–20 method, the electrode positions for the EEG were Cz, which are the predominant areas of CNV, and Pz, which is the predominant area of P300, with AFz as the ground electrode and the left earlobe as the reference electrode. To exclude electrical noise associated with blinking, electrodes were affixed above and below the left eye, and the electro-oculogram was measured. To eliminate artifacts based on spatial independence, EEG measurements were also taken for Fz, F1, F2, C1, C2, P1, and P2.

The experimental protocol is shown in Figure 1. Four ERP measurements were taken before (pre-consumption), immediately after (Post 1), 40 min after (Post 2), and 80 min after (Post 3) the meal, and the SSS was administered before

each measurement. Blood glucose levels were measured once before and after each ERP measurement, and the mean value was used as the representative value at each measurement time. A previous study reported that intense sleepiness occurs after ingestion of high-sugar foods [10]. Therefore, the dietary load used in the high-sugar food ingestion group was white bread (two x 20 mm thick slices) and water (285 ml), which has a high glycemic index (GI) value indicating the increase in blood glucose levels due to different foods [11]. The control group received only water (285 ml). The low-sugar food ingestion group was given low-sugar bread (approximately 120 g) and water (285 ml) to control for food ingestion and dietary content, and to manipulate the carbohydrate content of the food. The total carbohydrate content of the bread in the high-sugar food ingestion group was approximately 63 g and the low-sugar food ingestion group was approximately 22 g. Eating and drinking were prohibited two hours prior to the start of the experiment, as well as the use of electronic devices, excessive exercise, eating, drinking, and sleeping outside of the measurement time.

The oddball paradigm and the CNV paradigm are widely used for P300-evoked and CNV-evoked tasks, respectively. In the oddball paradigm, subjects were randomly presented with two types of stimuli with different presentation frequencies and were asked to respond only to the stimulus presented at a lower frequency [6]. The CNVs were elicited by presenting the second stimulus (S2) 3–7 seconds after the first stimulus (S1) and requesting a possible behavioral response to S2. In this study, to measure P300 and CNV simultaneously, we employed two types of stimuli for S2 in the CNV paradigm: low-frequency and high-frequency stimuli (see Figure 2). S1 was a pure tone at 1,000 Hz, presented as an auditory stimulus through an earphone attached to the subject's ear; S2 was a visual stimulus presented through an LCD placed 60 cm in front of the subject. The visual stimuli were "A" and "B" images in the center of the LCD screen as the low-frequency and high-frequency stimuli, respectively. Participants were instructed to quickly press a button switch for the low-frequency stimulus.
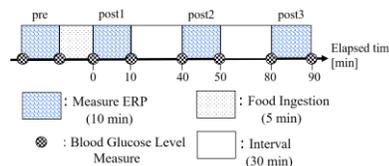
Figure 1.  Experiment protocol
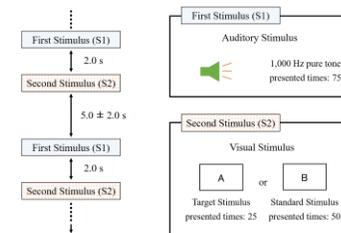
Figure 2.  Experimental paradigm

## III. ANALYSIS METHOD

### A. P300 Analysis

A 0.5–7 Hz bandpass filter was applied to the EEG data at Pz. EEG and electro-oculogram data were then extracted for five seconds before and after the stimulus presentation (10 seconds in total) during each target stimulus. The InfoMax ICA algorithm [12] was applied to the EEG data to remove artifacts associated with blinking, and components with correlation coefficients greater than $\pm 0.6$ with the electro-oculogram during the same time period were excluded. Finally, the baseline was corrected by subtracting the average voltage value during the 0.25 s before the presentation of the target stimulus. In the data of each EEG during target stimulation, we performed additive averaging, excluding trials in which the button switch was pressed incorrectly and where the voltage value exceeded $\pm 75$ µV in the interval from 0.2 s before to 0.8 s after the presentation of the target stimulus. In this study, we identified the positive peak above 2.5 µV that appeared 0.2–0.6 s after presentation of the target stimulus as P300, and derived the P300 latency. The calculated P300 latencies were compared using the Wilcoxon signed-rank test for each value before and after feeding. The significance level was set at $p < 0.05$. A typical waveform of P300 measured in the same subject is shown in Figure 3.

### B. CNV Analysis

For CNV derivation, EEG and EOG data at Cz from four seconds before S1 presentation to four seconds after S2 presentation (total 10 seconds) were extracted. To remove artifacts caused by blinking, the extracted EEG data were component decomposed with InfoMax ICA, and independent components with an absolute correlation coefficient of 0.7 or higher with the electro-oculogram at the same time were removed and reconstructed. The EEG data, excluding the effect of blinking, were baseline corrected by subtracting the average amplitude of 0.25 seconds before S1 presentation. For each of the above processed EEG data, an additive average was performed by excluding trials in which no button presses were observed within 0.5 seconds and trials in which the amplitude exceeded $\pm 75$ µV. In this study, the interval from 0.4 to 0.8 seconds after S1 presentation was defined as early CNV, and the interval from one second before S2 presentation to one second after S2 presentation as late CNV, and the mean amplitudes of these intervals were derived for each subject [13]. The mean amplitudes of the calculated CNVs were compared before and after feeding using the Wilcoxon signed-rank test for each value. The significance level was set at $p < 0.05$. A typical waveform of CNV measured in the same subject is shown in Figure 4.



Figure 3.   Typical waveform of P300 for one participant:
(a) high-sugar food ingestion group, (b) control group,
(c) low-sugar food ingestion group
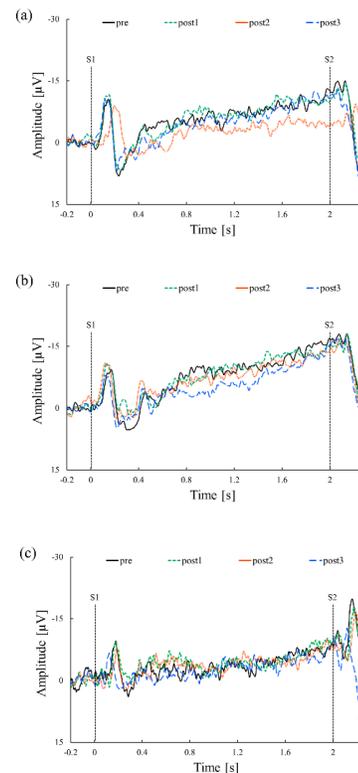


Figure 4.   Typical waveform of P300 for one participant:
(a) high-sugar food ingestion group, (b) control group,
(c) low-sugar food ingestion group

## IV.   RESULTS

Figure 5 shows the change over time of the mean value of each analytical index for all subjects.

The mean value of the SSS in the high-sugar food ingestion group was 2.5 for pre-intake, and significantly increased to 3.2 in Post 2 ($p < 0.05$). In the mean values of the SSS in the low-sugar food ingestion and control groups, there was no significant difference between the pre- and post-intake values when compared using Wilcoxon's signed rank test for the pre- and post-intake values, respectively.

Next, the mean reaction time from visual stimulus presentation to button press in the high-sugar food ingestion group was approximately 0.3 seconds at all measurement times, and the Wilcoxon signed-rank test showed no significant difference between the pre- and postprandial values. In the mean reaction time from visual stimulus presentation to button press in the low-sugar food ingestion group and the control group, a comparison using Wilcoxon's signed-rank test between the pre- and postprandial values showed no significant difference between them. Two out of 10 subjects in the low-sugar food ingestion group were excluded from the analysis because the button switch did not work properly.

Next, the mean value of P300 latency in the high-sugar food ingestion group was approximately 0.33 seconds for pre-intake, but was significantly longer in Post 2, approximately 0.36 seconds ($p < 0.05$). In the mean value of P300 latency in the low-sugar food ingestion and control groups, there was no significant difference between pre and post-intake when compared using Wilcoxon's signed rank test for each value in the pre- and post-intake groups.

Next, the mean amplitude of the preprimary CNV in the high-sugar food ingestion group was approximately -2.5 µV for the pre-intake, but significantly increased to about -1.1 µV in Post 2 ($p < 0.05$). In the mean amplitude of the early CNV in the low-sugar food ingestion and control groups, there was no significant difference between the pre- and post-intake values when compared using Wilcoxon's signed rank test for each value in the pre- and post-intake groups.

Next, the mean amplitude of late CNV in the high-sugar food ingestion group was approximately -5.2 µV for pre-intake, but significantly increased to about -2.9 µV in Post 2 ($p < 0.05$). In the mean amplitude of late CNV in the low-sugar food ingestion and control groups, there was no significant difference between pre- and post-intake values when compared using Wilcoxon's signed rank test for each value in the pre- and post-intake groups.

The mean blood glucose level in the high-sugar food ingestion group was 97 mg/dL for pre-intake, but significantly increased to 114 mg/dL in Post 1 and 145 mg/dL in Post 2 ($p < 0.05$). Blood glucose levels in Post 2 were significantly higher than those in Post 1 and Post 3 ($p < 0.05$) (see Figure 6). The mean values of blood glucose in the low-sugar food ingestion group showed no significant difference between the pre- and postprandial values using Wilcoxon's signed rank test.

In Post 1, blood glucose significantly increased from 99.7 mg/dL before ERP measurement to 128.8 mg/dL after ERP

measurement ($p < 0.05$). The blood glucose level decreased significantly from 152.7 mg/dL before ERP measurement ($p < 0.05$) (see Figure 7).

The mean blood glucose level of all subjects in the low-sugar food ingestion group was 92.5 mg/dL after ERP measurement compared to 99.1 mg/dL before ERP measurement in Post 2, showing a significant decrease in blood glucose level ($p < 0.05$) (see Figure 7).
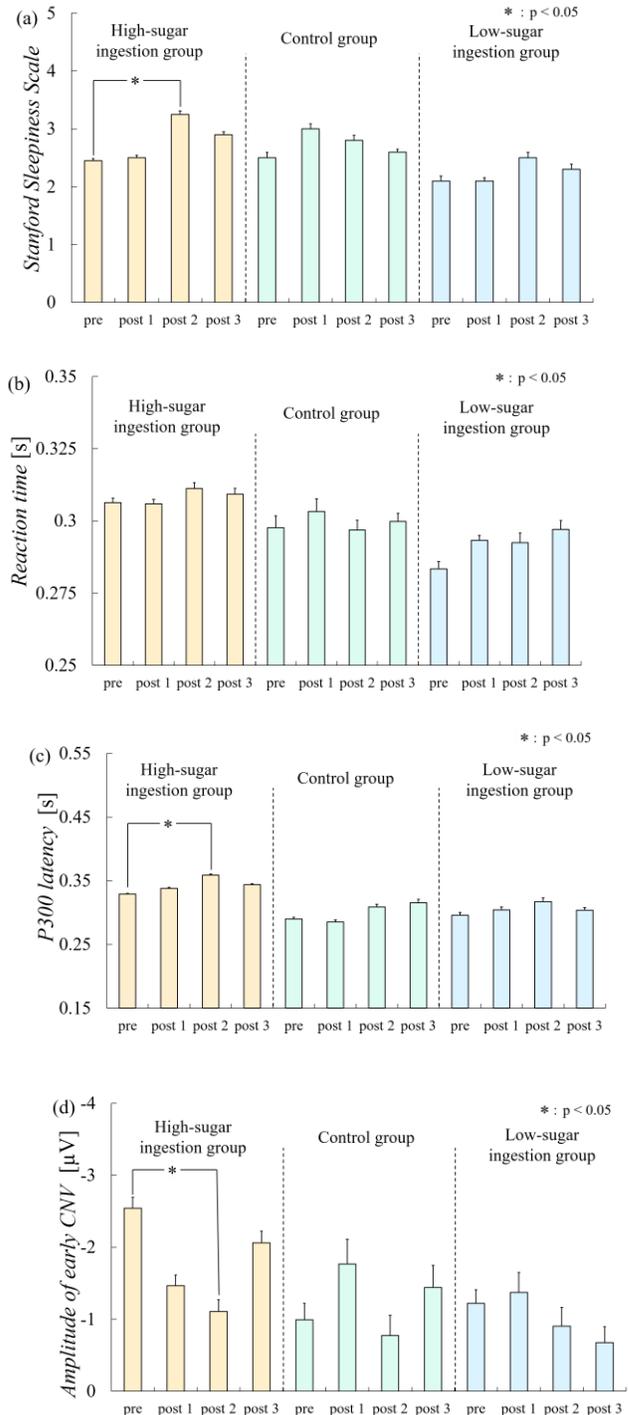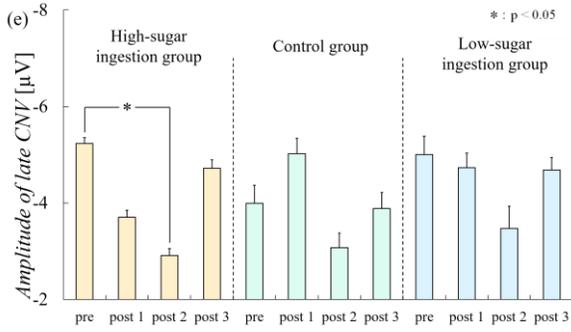
Figure 5. Change over time in each analytical index (Mean ± SE), (a) stanford sleepiness scale, (b) reaction time, (c) P300 latency, (d) amplitude of early CNV; (e) amplitude of late CNV



Figure 6. Change over time in blood glucose level (Mean ± SE)



Figure 7. Blood glucose level before and after ERP measurement (Mean ± SE);(a) High-sugar food ingestion group, (b) Low-sugar food ingestion group

## V. DISCUSSION

Recent research hypotheses that link postprandial brain dysfunction to fluctuations in blood glucose levels have been proposed to explain the pathogenesis of PLD, and have attracted much attention. Although blood glucose spikes and neuropeptide inhibition are representative examples of such hypotheses, the mechanism of PLD remains to be elucidated. This is due to the fact that there have been few cases in which the decline in brain function caused by postprandial sleepiness has been evaluated using quantitative indices, and where brain function and blood glucose levels before and after eating have been recorded simultaneously. In this study, we investigated the relationship between postprandial brain function decline and blood glucose level fluctuations by measuring ERP and blood glucose levels before and after consumption of two foods with different carbohydrate contents.

In the high-sugar food ingestion group that consumed white bread, a high GI food, there was an increase in the subjective sleepiness score, prolonged P300 latency, and increased early and late CNV amplitude in Post 2 compared to pre-intake. In addition, blood glucose levels measured at the same time were significantly increased in the high-sugar food ingestion group in Post 1 and Post 2 compared to pre-intake. In contrast, there were no significant changes in any of the parameters in the low-sugar food ingestion group before and after the meal. In 1990, Pivonka et al. evaluated postprandial sleepiness after consumption of high-sugar beverages and water using the SSS [14]. The results showed that the group that consumed high-sugar beverages had significantly increased values on the SSS compared to the group that consumed only water. This is consistent with the results of this study, in which PLD was observed only in the high-sugar food ingestion group with significantly increased blood glucose levels. In 2019, Ogata et al. also fed 20 university students with high- or low-GI foods and compared the number of students who fell asleep during lectures after lunch [15]. Ogata et al. also recorded blood glucose levels after lunch using a CGM, similar to this study. The results showed that blood glucose levels increased significantly when students consumed low-GI foods compared to when they consumed high-GI foods. In contrast, the number of students who dozed off during the lecture after lunch did not change even when the GI values of the foods were varied. However, Ogata et al. used the presence or absence of nodding off during lectures as an evaluation index for post-lunch sleepiness, and did not use a quantitative index to evaluate the post-lunch decline in brain function. In this study, in addition to the subjective questionnaire and blood glucose level, we measured ERPs, which were suggested to be useful as quantitative evaluation indices for postprandial brain function decline. As a result, ERP fluctuated significantly with a significant increase in blood glucose level only when high GI foods were consumed, confirming the decline in brain function. Therefore, this study's use of a quantitative evaluation index for postprandial decline in brain function provides new results that support the research
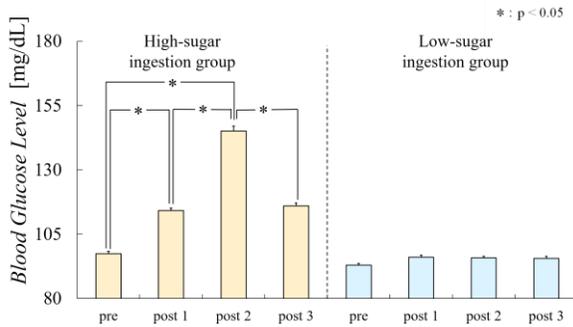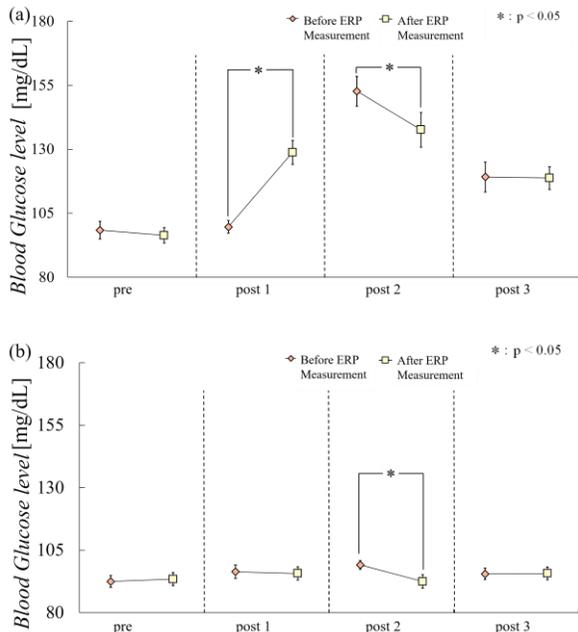
hypothesis that postprandial blood glucose fluctuations affect brain function.

In the high-sugar food ingestion group, there was a significant increase in blood glucose levels in Post 1 and Post 2 compared to pre-intake. However, increased subjective sleepiness and decreased brain function were not observed in Post 1, but only in Post 2. One of the major research hypotheses explaining the mechanism of PLD is the explanation by neuropeptide inhibition, which is a neuropeptide that regulates arousal level. One of the major research hypotheses to explain the mechanism of PLD, the explanation by suppression of neuropeptides, proposes that PLD is caused by the suppressed secretion of orexin, a neuropeptide that controls arousal level [5]. It is known that orexin secretion is inhibited in response to the degree of blood glucose elevation [16]. Therefore, the inhibitory effect of orexin is small at the degree of elevation of blood glucose level that occurred in Post 1 of this study, and it is considered that brain function did not decrease.

In addition, to investigate the tendency of blood glucose fluctuation during ERP measurement, blood glucose levels before and after ERP measurement were compared in this study. The results showed a significant increase in blood glucose levels before and after ERP measurement in Post 1, and a significant decrease in blood glucose levels before and after ERP measurement in Post 2 in the high-sugar food ingestion group. Therefore, PLD is thought to occur when blood glucose levels fall, not when they rise. The blood glucose spike explanation is a research hypothesis which posits that PLD is caused by the secretion of melatonin, which has hypnotic effects, in association with the additional secretion of insulin in response to the postprandial rise in blood glucose [4]. In other words, in the blood glucose spike explanation, PLD is thought to occur from the peak to the fall of blood glucose levels, when insulin secretion is prominent. In this study, PLD was also observed in Post 2, when blood glucose levels tended to decrease, and these experimental results support the blood glucose spike explanation. However, even in the low-sugar food ingestion group, where brain function did not decline after consumption, a significant decrease in blood glucose levels was observed before and after ERP measurement in Post 2. Therefore, it is possible that the postprandial decline in brain function does not necessarily occur when blood glucose levels fall, but rather when blood glucose levels fall after a postprandial increase to a high level.

## VI. CONCLUSION

To elucidate the pathogenesis of PLD, it is important to establish a quantitative evaluation index to assess brain dysfunction caused by eating. Currently, the hypothesis that PLD is caused by an increase in postprandial blood glucose level is sup-ported as a possible explanation for the pathogenesis of PLD. However, few studies have simultaneously measured postprandial brain dysfunction and blood glucose levels, and examined the relationship between the two. In this study, we measured blood glucose levels and ERP before and after consumption of two types of foods with different carbohydrate contents, and examined the relationship between postprandial blood glucose fluctuations and PLD.

The results showed that the SSS values increased significantly in the high-sugar food ingestion group in Post 2 compared to pre-intake. The SSS significantly in-creased in Post 2. The P300 latency was significantly prolonged in Post 2, and the early and late CNV amplitudes were significantly increased in Post 2. However, in the control group without food, there were no significant changes in any of the parameters before or after drinking. Therefore, P300 and CNV are highly useful as quantitative indices to evaluate the transient decline in brain function caused by PLD. There were no significant differences in subjective sleepiness, brain function, or blood glucose levels before and after eating in the low-sugar food ingestion group. In contrast, there was a significant increase in blood glucose levels in the high-sugar food ingestion group with impaired brain function in Post 1 and Post 2 compared to pre-, and a peak increase in blood glucose levels was observed in Post 2. Therefore, it was suggested that the postprandial rise in blood glucose was related to the expression of PLD. In the Post 2 blood glucose levels in the high-sugar food ingestion group, there was a significant decrease after ERP measurement compared to before ERP measurement. This suggests that PLD occurs during hyperglycemia and when blood glucose levels fall.

In the future, we will investigate the relationship between blood glucose and brain function decline in detail, such as when moderate GI foods are consumed and when multiple foods are consumed. If we can clarify the conditions under which PLD is induced by blood glucose levels, it will be possible to estimate the amount of food consumed and the way of eating that reduces the decline in performance after a meal. These research results can be applied to various fields, such as sports science and nutritional science. Furthermore, we aim to establish systematic evaluation criteria for PLD and transient decline in brain function by conducting continuous experiments using the number of chews and the amount of food consumed as factors.

### REFERENCES

[1] A. Craig, "Acute effects of meals on perceptual and cognitive efficiency," Nutrition Reviews. vol. 44(3), pp. 163–171, 1986.

[2] J. Rutenfranz and W. P. Colquhoun, "Circadian rhythms in human performance, Scandinavian journal of work," environment & health, vol. 5(3), pp. 167–177, 1979.

[3] S. Garbarino, L. Nobili, M. Beelke, F. De Carli, and F. Ferrillo, "The Contributing Role of Sleepiness in Highway Vehicle Accident," Sleep, vol. 24(2), pp. 203–206 ,2001.

[4] A. Afaghi, H. O'Connor, and C. M. Chow, "High-glycemic-index carbohydrate meals shorten sleep onset," The American journal of clinical nutrition, vol. 43(1), pp. 25–35, 2003.

[5] L. A. Panossian and S. C. Veasey, "Daytime Sleepiness in Obesity: Mechanisms Beyond Obstructive" Sleep Apnea—A Review. Sleep, vol. 35(5), pp .605–615,2012.

[6] K. Nagano, K. Fumiya, amd T. Hideaki, "Quantitative Evaluation of Post-Lunch Dip Using Event-Related Potential," Journal of Advanced Computational Intelligence and Intelligent Informatics, vol. 26(1), pp. 67–73, 2022.

[7] H. Nittono, "Event-related potentials (ERPs) and cognitive activity: A new perspective from engineering psychology," Behavioral science research, vol. 42(1),pp. 25–35, 2003.

[8] T. Bailey, B. W. Bode, M. P. Christiansen, L. J Klaff, and S. Alva, "The Performance and Usability of a Factory-Calibrated Flash Glucose Monitoring System," Diabetes technology & therapeutics, vol. 17(11), pp. 787–794, 2015.

[9] J. R. Castle and W. K. Ward, "Amperometric glucose sensors: Sources of error and potential benefit of redundancy," Journal of diabetes science and technology, vol. 4(1), pp.221–225 ,2010.

[10] A. Smith, A. Ralph, and G. McNeill, "Influences of meal size on post-lunch changes in performance efficiency, mood, and cardiovascular function," Appetite, vol. 16(2), pp. 85–91,1991.

[11] K. Foster-Powell, S. H. Holt, and J. C. Brand-Miller, "International table of glycemic index and glycemic load values," Am. J. Clin. Nutr, vol. 76(1), pp. 5–56, 2022.

[12] A. Delorme and S. Makeig, "EEGLAB: An open source toolbox for analysis of single-trial EEG dynamics including independent component analysis, J. Neurosci. Methods, vol.134(1), pp. 9–21 2004.

[13] A. Delorme and S. Makeig, "EEGLAB: An open source toolbox for analysis of single-trial EEG dynamics including independent component analysis, J. Neurosci. Methods, vol.134(1), pp. 9–21 2004.

[14] Y. Nageishi, T. Shimura, and M. Shimokochi, "The Three Sub-Components of the Contingent Negative Variation," Bulletin of The Faculty of Human Sciences Osaka University, vol. 10, pp. 225–243, 1991.

[15] E. E. Pivonka and K. K Grunewald, "Aspartame- or sugar-sweetened beverages: effects on mood in young women," Journal of the American Dietetic Association, vol. 90(2), pp.250–255, 1990.

[16] N. Ogata and K. Masaki, "Lunch suggestion for improving learning attitude in the afternoon. Annual report of the Institute of Living and Environmental," Sciences, vol. 51, pp. 21–30, 2019.

[17] T. Sakurai, The Science of Sleep. 2nd edn. Koudansha Ltd, Japan 2017.

# Recruiting Neural Field Theory for Motor Imagery Data Augmentation

Daniel Polyakov

Department of Cognitive and Brain Sciences
Agricultural, Biological, Cognitive Robotics Initiative
Ben-Gurion University
Be'er Sheva, Israel
e-mail: polydani@post.bgu.ac.il

Oren Shriki

Department of Cognitive and Brain Sciences
Department of Computer Science
Ben-Gurion University
Be'er Sheva, Israel
e-mail: shrikio@bgu.ac.il

*Abstract*—**Brain-computer interfaces accuracy is often limited due to a lack of diverse training data. In this study, we face this problem by using a computational model of neural dynamics, specifically Neural Field Theory, to generate artificial electroencephalogram time series as additional training data. We fitted this model to common spatial patterns of each motor imagery class, jittered the fitted parameters, and augmented the training data by generating time series from the model. We then applied a linear discriminant analysis to classify motor imagery states based on total-power features and tested the accuracy improvement on the '2a' data set from brain-computer interfaces competition IV. Our findings show that data augmentation using Neural Field Theory can significantly improve the accuracy of brain-computer interface classifiers when the number of training samples is limited, providing a biophysically meaningful signal.**

*Keywords: brain-computer interface, neural field theory, data augmentation, motor imagery, EEG.*

## I. INTRODUCTION

Brain-Computer Interfaces (BCIs) allow for controlling computer and robotic applications directly with brain activity. A common problem in BCI systems is poor classification accuracy due to a lack of diverse training data, which is typically collected during tedious calibration sessions. Training data augmentation is a possible solution to this problem. Previous studies have explored various techniques, such as Ensemble Empirical Mode Decomposition (EEMD) [1] and spectral noising [2], to augment Motor Imagery (MI) electroencephalogram (EEG) signals.

Here we harness Neural Field Theory (NFT), a computational model of neural dynamics, to augment MI training data. NFT is a powerful method for constructing models of large-scale brain activity based on physiological principles. These models can be fitted to experimental EEG spectra and generate artificial time series accordingly [3], [4].

The rest of the paper is structured as follows. Section II presents the materials and methods used in this study. In Section III, we present the results obtained from our research. Section IV analyzes these results and compares them to other works in the field. Finally, in Section V, we draw conclusions based on our findings and provide directions for future research.

## II. MATERIALS AND METHODS

We applied Common Spatial Patterns (CSP) to the MI EEG epochs and computed the Total Power (TP) and Higuchi Fractal Dimension (HFD) of the CSPs. NFT models were fitted to each CSP time series of each MI class. The fitted parameters were jittered and artificial CSP signals were generated from the models. Linear Discriminant Analysis (LDA) was used to classify MI states based on TP and HFD features. To compare the effectiveness of our augmentation method, we also performed a naive augmentation by adding Gaussian noise to feature values.

We evaluated the accuracy improvement of our augmentation method on the '2a' data set from BCI competition IV, which consisted of 18 subjects performing right and left hand MI [5]. To imitate a small training set, we randomly divided each subject's data into three equal folds and used the first fold for training and NFT augmentation, and the other two folds for validation (as shown in Fig. 1).

## III. RESULTS

Our goal was to reach the classification accuracy of the full training set, by augmenting the small training set. In the case of TP-based classification, our data augmentation method increased the accuracy of the small training set from $\kappa=0.79$ (Cohen's Kappa [6]) to $\kappa=0.83$, surpassing the accuracy of the full training set ($\kappa=0.82$). In comparison, an augmentation that was done by noising the features decreased the accuracy to $\kappa=0.76$. For HFD-based classification, our augmentation method did not result in any improvement in accuracy. Please refer to TABLE I for complete results.

TABLE I. VALIDATION CLASSIFICATION ACCURACY $\kappa$ [a]

|  | *Full training set* | *Small training set* | *Small training set + NFT augmentation* | *Small training set + noise augmentation* |
|---|---|---|---|---|
| TP feature | 0.82 | 0.79 | 0.83 | 0.76 |
| HFD feature | 0.89 | 0.86 | 0.84 | 0.84 |

a. Inter-subject average

## IV. DISCUSSION

Our results demonstrate that the NFT-based data augmentation technique effectively improved the

classification accuracy to the level of a full training set, enabling the use of shorter MI training sessions. The improvement was evident for TP-based classification but not for HFD-based, suggesting that NFT generates EEG signals that better preserve spectrum-based features compared to time-domain-based features.

This augmentation technique outperformed the noise-based augmentation method. This may be attributed to the physiological realism of the NFT-generated signals, which resemble real EEG signals and are distributed in a biophysical manner in a physiologically valid range.

Its performance was at similar levels to the state-of-the-art augmentation methods mentioned before. EEMD-based augmentation increased the accuracy from $\kappa=0.66$ to $\kappa=0.82$, while spectral noising increased in from $\kappa=0.65$ to $\kappa=0.68$, both on the '2a' data set [1], [2]. A direct comparison is not feasible due to varying initial accuracy levels and evaluation methods in the studies.

## V.    CONCLUSION AND FUTURE WORK

In this study, we addressed the challenge of limited training data in BCIs by proposing a novel augmentation approach. We used NFT to fit a physiological model to MI EEG signals and generated diverse artificial data for training. Our approach improved the accuracy of MI-based BCI classifiers and provided biophysical meaning to the generated signals. Overall, our findings suggest that data augmentation using NFT can be an effective solution for improving BCI performance when the number of training samples is limited. To assess the generalizability of our method, the next step would be to evaluate its performance on other BCI paradigms, such as Steady State Visual Evoked Potentials (SSVEP) and P300. This would help determine if our results can be extended to other BCI applications.

REFERENCES

[1]  H. K. Lee, J. H. Lee, J. O. Park, and Y. S. Choi, "Data-driven Data Augmentation for Motor Imagery Brain-Computer Interface," in International Conference on Information Networking, Jan. 2021, pp. 683–686. doi: 10.1109/ICOIN50884.2021.9333908.

[2]  X. Zhang, M. Lei, and Y. Li, "An amplitudes-perturbation data augmentation method in convolutional neural networks for EEG decoding," 2018 5th Int. Conf. Information, Cybern. Comput. Soc. Syst., pp. 231–235, 2018.

[3]  P. A. Robinson, C. J. Rennie, D. L. Rowe, S. C. O'Connor, and E. Gordon, "Multiscale brain modelling," Philos. Trans. R. Soc. B Biol. Sci., vol. 360, no. 1457, pp. 1043–1050, 2005, doi: 10.1098/rstb.2005.1638.

[4]  R. G. Abeysuriya and P. A. Robinson, "Real-time automated EEG tracking of brain states using neural field theory," J. Neurosci. Methods, vol. 258, pp. 28–45, Jan. 2016, doi: 10.1016/j.jneumeth.2015.09.026.

[5]  M. Tangermann et al., "Review of the BCI competition IV," Front. Neurosci., vol. 6, no. July, pp. 1–31, 2012, doi: 10.3389/fnins.2012.00055.

[6]  J. Cohen, "A Coefficient of Agreement for Nominal Scales," Educ. Psychol. Meas., vol. 20, no. 1, pp. 37–46, 1960, doi: 10.1177/001316446002000104.
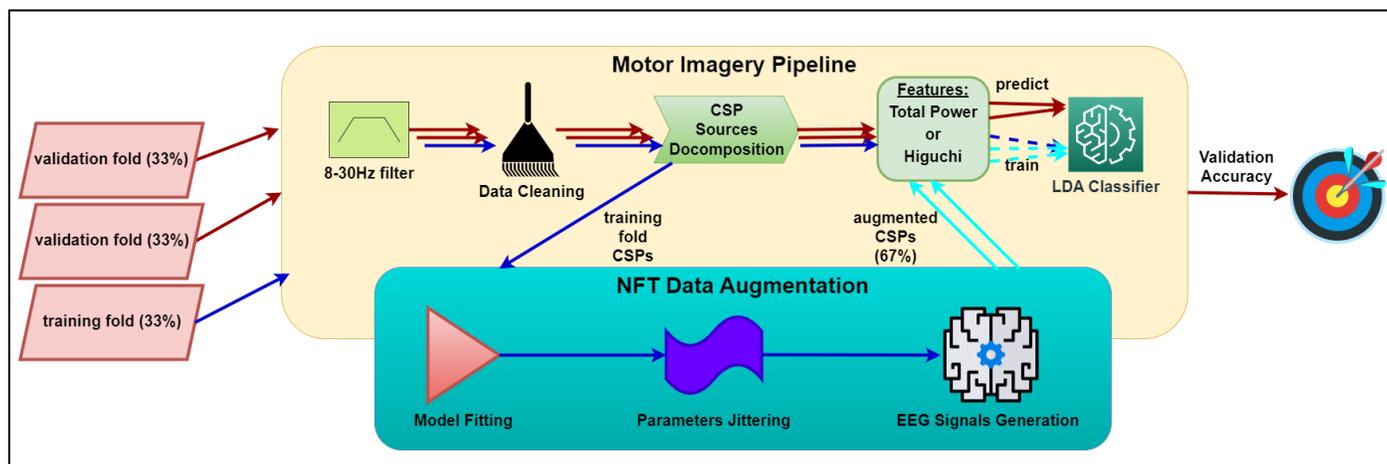


Figure 1.  MI data augmentation performance evaluation procedure flow.

# Social Context Impacts Brain Activation Pattern during Visual Perception of Movement: an fMRI Study

Marie Chudožilov Bendová
Third Faculty of Medicine, Charles University
Prague, Czechia
Email: mariebendova42@gmail.com

Alexandra Morozova
Third Faculty of Medicine, Charles University
Prague, Czechia
National Institute of Mental Health, Klecany, Czechia
Laboratory of Motor Control, University of Milan
Milan, Italy
Email: alexandra.morozova@lf3.cuni.cz

Luciano Simone
Department of Medicine and Surgery, Università di Parma
Parma, Italy
Email: luciano.simone@unipr.it

Zhanna Garakh
Institute of Higher Nervous Activity and Neurophysiology of
Russian Academy of Sciences
Moscow, Russia
Email: garakh@yandex.ru

Yuliya Zaytseva
Third Faculty of Medicine, Charles University
National Institute of Mental Health
Prague, Czechia
Email: yuliya.zaytseva@gmail.com

*Abstract*—**Perception of biological movements is integral to one's ability to interpret actions of others. In the present study, we conducted a comparative analysis of neural responses in a functional Magnetic Resonance Imaging (fMRI) setting during visual perception of biological movement within a social context (which has not been studied yet) as opposed to a non-biological baseline stimulus. Our results demonstrate right lateralization of superior temporal Region Of Interest (ROI), likely reflecting the underlying differences in social characteristics of each given stimulus.**

*Keywords - functional magnetic resonance imaging; movement perception; biological movement; social movement.*

## I. INTRODUCTION

The movements of living beings provide rich and meaningful information that facilitates social interaction. Despite improved understanding of the brain regions involved in social behavior and its perception, the details of neural representations require further experimental and theoretical work. The neurofunctional differences between different types of biological movement may serve for interpretation of one's immediate intentions. This study comprised a comparative analysis of neural responses in an fMRI setting during visual perception of different types of biological movement with and without social context.

The rest of the paper is structured as follows. In Section II, we present the methods. In Section III, we show the results. In Section IV, we discuss the outcomes. Finally, Section V concludes the work.

## II. METHODS

20 healthy subjects aged 21 to 31, IQ > 85, were scanned on a 3-T Prisma scanner at the National Institute of Mental Health in Klecany, Czech Republic. The study was approved by the local ethical committee. The fMRI block design paradigm included two sessions with all stimuli presented twice; the order of stimuli was counterbalanced across subjects. All participants observed three types of biological movement within different social contexts (single hand, fist, and a handshake) and a control stimulus (a stationary cross).

Data analysis was executed in the Statistical Parametric Mapping (SPM) software [1]. Whole brain analysis as well as ROI analysis were applied to address brain activations under each condition. The areas selected for the ROI analysis (precentral, superior, and inferior temporal and parietal gyrus bilaterally) were based on predefined brain structures that are involved in movement processing as well as social perception [2][3].

## III. RESULTS

### A. Whole Brain Analysis

The observation of all stimuli elicited activation in the frontal, parietal, and occipital-temporal regions involved in visual movement perception (see Table 1). Bigger cluster size and a higher Z-score correspond to increased activity in the peak area.

### B. ROI analysis

ROI-based analysis highlighted cluster differences. Figures 1-3 depict the activation pattern overlap upon presenting the biological stimuli. The inferior parietal (Fig.2) and the precentral gyrus (Fig.1) were more active in the left hemisphere, while the superior temporal gyrus (Fig.3) showed right lateralization.

## IV. DISCUSSION

The current study compared neural responses of three types of biological movement. Right hemisphere lateralization was previously documented [4], and the brain

areas that elicited higher activity go in line with several studies [4][5]. However, Sokolov et al. [6] did not find substantial activation in the inferior parietal gyrus, contrary to our findings, likely due to the difference between presented stimuli.

## V.    CONCLUSION

Our results showed that the right-lateralized superior temporal ROIs were more selective in response to the presented visual cues, likely reflecting the underlying differences in social characteristics of each given stimulus. This provides further insight into the neurobiology of social movement perception and may serve as a baseline for future studies.

## ACKNOWLEDGMENT

## REFERENCES

[1]  K. J. Friston, J. T. Ashburner, S. J. Kiebel, T. E. Nichols, and W. D. Penny, "Statistical Parametric Mapping: The Analysis of Functional Brain Images." Elsevier/Academic Press, 2007.

[2]  J. C. Thompson, M. Clarke, T. Stewart, and A. Puce, "Configural processing of biological motion in human superior temporal sulcus", J. Neurosci, vol. 25(39), pp. 9059-66, Sep 2005.

[3]  M. H. Grosbras, S. Beaton, and S. B. Eickhoff, "Brain regions involved in human movement perception: a quantitative voxel-based meta-analysis", Hum Brain Mapp, vol. 33(2), pp. 431-54, Mar 2011.

[4]  J. Grèzes, P. Fonlupt, B. Bertenthal, C. Delon-Martin, C. Segebarth, and J. Decety, "Does perception of biological motion rely on specific brain regions?" Neuroimage, vol. 13(5), pp.775-785, May 2001.

[5]  L. M. Vaina, J. Solomon, S. Chowdhury, P. Sinha, and J. W. Belliveau, "Functional neuroanatomy of biological motion perception in humans", Proc Natl Acad Sci USA, vol. 98(20):11656-61, Sep 2001.

[6]  A. A. Sokolov, P. Zeidman, M. Erb, P. Ryvlin, K. J. Friston, and M.A. Pavlova, "Structural and effective brain connectivity underlying biological motion detection", Proc Natl Acad Sci USA, vol. 115(51):E12034-E12042, Dec 2018.
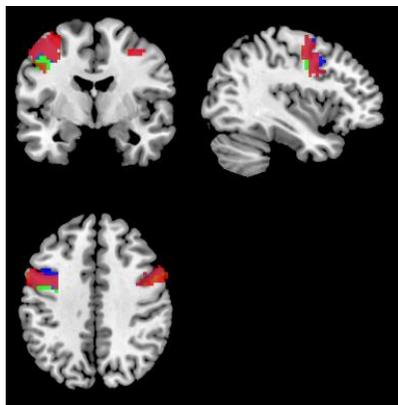


Figure 1. Precentral gyrus activation.
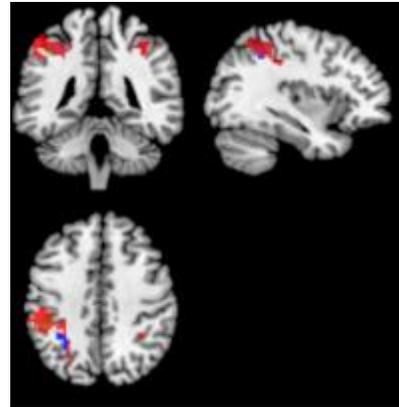


Figure 2. Inferior parietal gyrus activation.
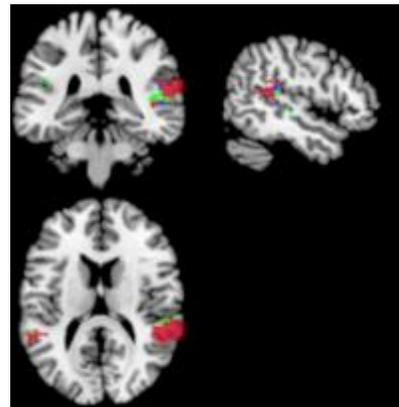


Figure 3. Superior temporal area activation.

Legend: Green – hand vs cross, Red – fist vs cross, Blue – handshake vs cross

TABLE I.        WHOLE BRAIN ANALYSIS

| Stimulus | Cluster size (voxels) | Z score | Peak | | | p(FWE) | Peak area |
|---|---|---|---|---|---|---|---|
| | | | x | y | z | | |
| Hand vs. cross | 5074 | 6.23 | -48 | -76 | -5 | < 0.001 | Middle Occipital L |
| | 400 | 4.74 | -36 | -4 | 50 | < 0.001 | Precentral L |
| | 296 | 4.36 | 42 | 5 | 47 | < 0.001 | Precentral R |
| | 266 | 4.21 | 27 | -67 | 38 | < 0.001 | Superior Occipital R |
| Fist vs. cross | 6696 | 6.32 | 39 | -67 | -16 | < 0.001 | Fusiform R |
| | 764 | 05.09 | 51 | 5 | 47 | < 0.001 | Precentral R |
| | 444 | 05.01 | -51 | 8 | 41 | < 0.001 | Precentral L |
| Handshake vs. cross | 5418 | 06.04 | 39 | -61 | -7 | < 0.001 | Inferior Temporal R |
| | 489 | 05.01 | 42 | 5 | 50 | < 0.001 | Precentral R |
| | 415 | 4.71 | -42 | 5 | 41 | < 0.001 | Precentral L |
| | 201 | 4.24 | 30 | -46 | 50 | 0.001 | Inferior Parietal R |

# A Postulate: Connectome Development is the Driving Factor of Brain Growth

Michael Bihn
*Dept. of Computer Science*
*University of Colorado at Colorado Springs*
Colorado Springs, USA
email: mbihn@uccs.edu

Rory Lewis
*Dept. of Computer Science*
*University of Colorado at Colorado Springs*
Colorado Springs, USA
email: rlewis5@uccs.edu

*Abstract*—We postulate that the consensus architecture inherent in the Common Model of Cognition (CMC) not only captures decades of progress in cognitive science and modeling human and human-like intelligence, but that the CMC also connects and strengthens the idea that brain growth is directly correlated to connectome development. In this paper, we show how these relationships are driven by the development of the communication links, the synapses, between the axon and the dendrite, hence providing interneuronal communication, in essence, we show how these are driven by the connectome development. We provide a mathematical means for defining brain growth of the grey matter layers, lobes and the white matter pathways.

*Keywords*—connectomes; fetal brain development; artificial intelligence.

## I. Introduction

We postulate that, because it is commonly accepted that common sense in humans and animals requires priori and posterior knowledge [1], if one were to synthesize a mechanism to store priori and posterior knowledge, one would need to mathematically emulate steps in neuroscience that map the development of the fetal brain from conception to two years of age. This mapping will include, but is not limited to i) emulating how the directionality of brain signals in the white matter of the brain form a plurality of synaptic pathways [2], that enable a flow of information between distant gray matter regions [3], ii) presenting a modular network topology in the brain from the first days of life [4] [5], and iii) adhering to the recent mapping of the human connectome [6] [7].

Herein, we postulate the ability of tracking infantile brain development over time. Using data collected from the baby connectome project [8], we will derive the growth rates and accelerations of the brain regions of grey matter and the pathways of the white matter. The resulting growth rates and accelerations along with their time of occurrence provide us with a sequence of events in the infantile brain development. The resulting sequences are then utilized as a script for the brain model development, defining which Regions of Interest (ROI), layers and pathways are deployed, when and where. Accordingly, we present the first step towards building a developing model reflecting the infant human brain development. This model provides the physical structure of the brain's development, laying out which structures are available to learn functionality over time. Thus, the functionality can only be learned if the physical structure exists and the actual neurons are trained with posterior experience leading to knowledge. Because we are limited by the data available, the specific experiences over time from conception to two years of age are not available. Hence, our model is limited to physical growth until experiential data is tracked for subjects.

The rest of this paper is structured as follows. In section II, we discuss brain development. In section III, we explain our dynamic modeling of brain growth. In section IV, we discretize growth into solvable problems. In section V, we present our conclusion and future work.

## II. Brain Development

Recent research in brain development centers on how a first set of neurons that become grey matter grow radially outward before a second set of neurons that will form white matter pathways, grow tangentially underneath the first set of neurons and consequently pushes it outward [9] [10] [11] [12]. In the first six months of fetal growth the brain is driven by genetic influences [11] including developments in the womb that are more priori than posteriori. Zollei *et al.* [13] found myelin accumulation was critical in the development in the fetus brain, that included 14 white matter pathways, increased fractional anisotropy (FA), and decreased mean diffusivity (MD). After the first six months, the brain continues to develop its white matter pathways up the 42 known bundles [14] in the adult.

### A. Recent Brain Atlas Research

In order to appreciate our contribution to optimizing brain atlas research we review the state-of-the-art in this field. In building a more efficient and accurate pediatric brain atlas we model the lobe and pathway development from instantiation through 2 years of age by leveraging 4D surfaces introduced by Li *et al.* [15] where separate surfaces were created for various intervals of time from birth to 24 months of age. Our model is unique from Li *et al.*'s 4D surfaces because we include pathways and their connections in our model. We note that Maffei *et al.* [14] developed a pathway atlas they integrated it into their TRACULA; however, our model is unique from Maffei *et al.*'s work as we are particularly interested in the neurological growth from conception to two years of age. Our age range inherent in the mapping of our model also

differentiates us from work performed by Maier *et al.* [16] who refined pathway definitions from several researchers to produce ground truth for the fiber bundles. To effectively model the brain's growth, as alluded to above, we have differentiated space and time in order to observe the *rate and acceleration* of growth. Here, our model focused on keeping track of how the fetal brain grows. Fetal neuronal growth is complex and in order to effectively track said growth, the resulting system needs to track how the fetal brain produces 250,000 nerve cells every minute from conception to birth [11] that form pathways and six distinct compartments that become lobes. Our system tracks the brain lobes as they move through the brain. More so it will also track the new lobes appearance and their subsequent motion to their destination and track the pathways appearance and growth as they connect the lobes.

### B. Recent Common Model of Cognition Research

The Common Model of Cognition (CMC) not only captures decades of progress in cognitive science and modeling human and human-like intelligence as proposed by Stocco *et al.* , [17], but, as described in their paper, the CMC also connects and strengthens the idea that brain growth is directly correlated to connectome development. This view that the fetal brain's network develops in conjunction with the connectomes is well-supported by large-scale analysis of the human functional connectome. This paper adds to this concept because we show that it is commonly accepted that common sense in humans and animals requires priori and posterior knowledge which means that if one were to synthesize a mechanism to store priori and posterior knowledge, one would need to mathematically emulate steps in neuroscience that map the development of the fetal brain from conception to two years of age.

The CMC proposed by Laird *et al.*, [18] is comprised of a set of principles that summarize the similarities of multiple cognitive architectures that were developed over the course of five decades in the fields of cognitive psychology, artificial intelligence, and robotics [17]. The CMC has been used to design cognitive agents because agents exhibiting human-like intelligence share five functional components: a feature-based declarative long-term memory, a buffer-based working memory, a system for the pattern-directed invocation of actions represented in procedural memory, and dedicated perception and action systems. Importantly, the CMC has been used as a basis in computational neuroscience in robotics' AI system and artificial neural networks including but not limited to DeepMind's AlphaGo [17], look-ahead search, working memory and procedural memory, in addition to dedicated systems for perception and action [19] and the Differentiable Neural Computer [20]. Therefore, the cross-correlation between the CMC connecting robotics and the fetal brain deems it as a critical resource in validating connectomic perturbations and fetal brain growth,

### III. Dynamic modeling of Brain Growth

As mentioned above, we model the brain's growth by differentiating by space and time. Here, the space differentiation shall consider three differing structures, called 'spaces' of the brain, i) the grey matter, ii) the white matter and the iii) intersecting matter. In each space separate entities will be called out. For the grey matter space the entity distinction shall be the name of the brain lobe or layer. For the white matter space the entity distinction shall be the white matter pathway. For the intersecting matter the entity distinction shall be the combined pathway-lobe pair. Additionally, the intersecting matter represents the neuronal pathways terminating into grey matter lobes, a definite intermingling of volumes that shall be better defined by future research. We provide a location and volume description for each lobe in the grey space, each pathway in the white space, and each pathway-lobe pair in the intersecting matter, for each time instance, if the entity exist at that time. Additionally the pathway entities include the set of streamline definitions that comprise that particular pathway. The streamline definition includes the coordinates of each axonal segment found by MRI. With the longitudinal data of position and volume over time, Curve fittings shall provide the functions for individual entity volume growth and positional movement. These functions shall be integrated into a differential equation representing the position movement and a differential equation representing the volume growth for each of the lobes, pathways, and pathway-lobe pair. Further refinement of these spaces may be possible in the future.

### IV. Discretizing Growth into Solvable Problems

Our goal is to mathematically model the growth of the brain. There are quite a few facets to consider. The brain starts by building the layers of the grey matter and then builds the white matter connections underneath them. The layers of the grey matter development is different from the white matter development. Separate models will be developed and then combined. Both developments contribute to the brain volume growth. The grey matter development might take into consideration several factors including the neuronal growth, the movement towards the skull, the changes in density of the separate layer and the insertion of white matter pathway connections. The white matter development starts after the grey matter development. The white matter development is different from the grey matter development due the oligo-dendrocytes, glial cells, that excrete the myelin around the axons, producing the white. For each layer and for each pathway, a model will be developed as data becomes available from the connectome project. Several measures are currently used to describe the brain such as Fractional Anisotropy (FA), Mean Diffusivity (MD) [13], Cortical Thickness, surface area, gyrification, and position [15]. Therefore, longitudinal parameter and data values representing brain structure with collected data over time, are candidates for the same analysis we propose.

For instance, given the volume measurements collected over time, we can plot the volume over time and curve fit to

produce a function for volume over time. The challenge is locating the method for curve fitting is finding the method that minimizes error. With the function *VolumeOverTime*, we then take the first and second derivatives to give the growth rate and acceleration. This same approach can be applied to any brain measurements that have been collected. Myelination over time should be included for the white matter model. The sum of these functions provide the brain development model. There will be intersecting variables in these functions that will need to be resolved. Volume is dependent on density, which is dependent on the growth rate of the skull and its volume. First we have the total brain volume over time as the sum of the volumes of the grey matter layers volume and the sum of the white matter pathway volumes.

$$TV(t) = \sum (GLV_{t,i}, i = 1..14 + \sum (WPV_{t,j}, j1.. = 42) \tag{1}$$

where GLV is the grey matter layer volume for each of the fourteen grey matter layers and WPV is the white matter volume for each of the 42 white matter pathways. We take the derivative of both sides.

$$TV'(t) = \sum (GLV'_{t,i}, i = 1..14 + \sum (WPV'_{t,j}, j = 1..42) \tag{2}$$

where we now have GLV' as the growth rate of grey matter layers over time and WPV' as growth rate of the white matter pathways over time. These growth rates give the rates at which these distinguishable brain regions shall grow in our synthesis of the infantile brain development. We now take the second derivative.

$$TV''(t) = \sum (GLV''_{t,i}, i = 1..14 + \sum (WPV''_{t,j}, j = 1..42) \tag{3}$$

where we now have GLV'' as the acceleration of grey matter layer growth over time and WPV'' as acceleration of the white matter pathway growth over time. These accelerations give the time at which these distinguishable brain regions grow in our synthesis of the infantile brain development. From [10] [11] we know that these individual regions of interest develop in an almost prescribed order with certain functions taking precedence, such as vision and auditory. What we have defined here is a means to quantify the mathematical order of growth by using the accelerations and growth rates.

A region of interest or pathway starts growth with an acceleration of growth, from no existence to growth. When the growth is completed the acceleration and the growth rate falls back to zero. Therefore, we can determine the ordering over time of the infantile brain development. We show an example of the difference in growth between two regions of interest in Figure 1. In order to test our hypothesis, we generated random sample data to reflect differing rates of growth; the red region shows the volume difference of the two regions over time. If the curve fitting provides a mathematically twice differentiable function then a differential equation can be developed for the growth of a specific region over time. This will lead to the investigation of any patterns of development.
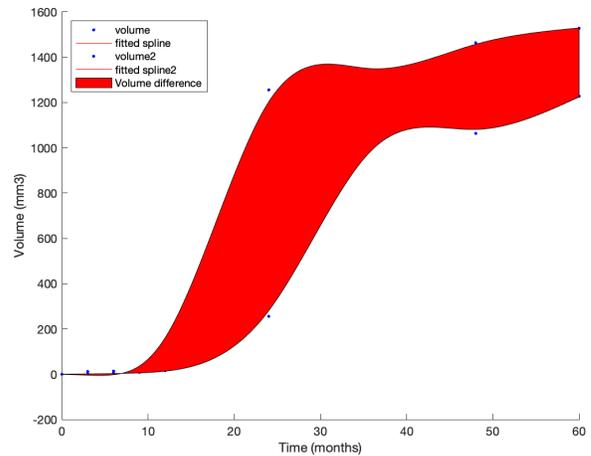


Fig. 1. The difference between two brain regions volume over time.

We show the growth rate and acceleration in Figure 2. The growth rate and acceleration must be positive going from no volume to the identified region. Our example used spline curve fitting which probably produced a piece-wise function that would not be friendly to differentiation for pattern investigation. This process could be expanded from conception to two years of age to death, possibly identifying the negative growth in dementia.
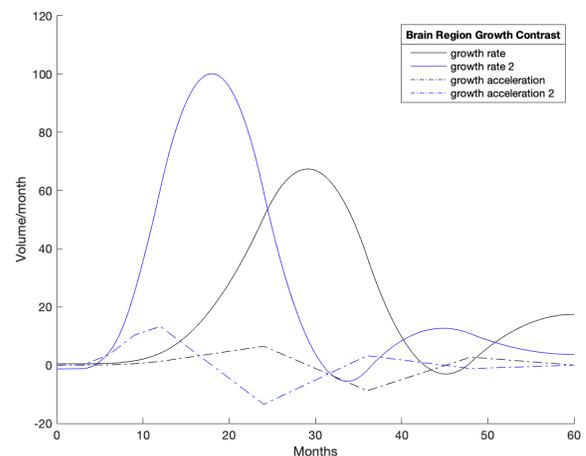


Fig. 2. The growth rate and acceleration between two brain regions over time.

## V. CONCLUSION AND FUTURE WORK

We have described how the brain growth model is inherently linked to connectome growth. It is generally accepted that Rapid cortical Gyrification Index (GI) and Local Gyrification Index (LGI) growth in the early postnatal period is related to 1) an increase of dendritic arborization [21] [10] and 2) growth of the terminal axon arborization, synaptogenesis [21]. We can logically determine that because all of the aforementioned

occurs inside of the fetal brain's connectome development, that these connectomes are therefore a major factor in determining fetal brain development *per se*. We therefore deduce that it will be interesting to investigate how the cortical LGI relates to the underlying WM connectivity. Lastly, while relationships have been established between several factors, it is our hypothesis that neuronal proliferation, and the glial proliferation providing the myelination for the axons, to protect their signals, are a contributing force in brain growth. The connectome model will contribute a means to efficiently define and predict brain growth not seen before. Furthermore, a second subset of our hypothesis is the aforementioned moves existing structures away from their origin to their predestined position in the brain.

## REFERENCES

[1] I. Kant, "The possibility of experience," *Journey into Philosophy: An Introduction with Classic and Contemporary Readings*, p. 42, 2016.

[2] F. Babiloni *et al.*, "Estimation of the cortical functional connectivity with the multimodal integration of high-resolution eeg and fmri data by directed transfer function," *Neuroimage*, vol. 24, no. 1, pp. 118–131, 2005.

[3] P. Bartolomeo, "The quest for the critical lesion site in cognitive deficits: problems and perspectives," *Cortex*, vol. 47, no. 8, pp. 1010–1012, 2011.

[4] P. Hagmann *et al.*, "Mapping human whole-brain structural networks with diffusion mri," *PloS one*, vol. 2, no. 7, p. e597, 2007.

[5] O. Sporns, *Networks of the Brain*. MIT press, 2010.

[6] Fischi-Gomez *et al.*, "Brain network characterization of high-risk preterm-born school-age children," *NeuroImage: Clinical*, vol. 11, pp. 195–209, 2016.

[7] A. Sokolov Arseny *et al.*, "Brain network analyses in clinical neuroscience," *Swiss Archives of Neurology, Psychiatry and Psychotherapy*, vol. 170, no. 6, 2019.

[8] B. R. Howell *et al.*, "The unc/umn baby connectome project (bcp): An overview of the study design and protocol development," *NeuroImage*, vol. 185, pp. 891–905, 2019.

[9] I. Kostović, G. Sedmak, and M. Judaš, "Neural histology and neurogenesis of the human fetal and infant brain," *Neuroimage*, vol. 188, pp. 743–773, 2019.

[10] G. Li *et al.*, "Mapping longitudinal development of local cortical gyrification in infants from birth to 2 years of age," *Journal of Neuroscience*, vol. 34, no. 12, pp. 4228–4238, 2014.

[11] L. Vasung *et al.*, "Exploring early human brain development with structural and physiological neuroimaging," *Neuroimage*, vol. 187, pp. 226–254, 2019.

[12] K. Xia *et al.*, "Genetic influences on longitudinal trajectories of cortical thickness and surface area during the first 2 years of life," *Cerebral Cortex*, vol. 32, no. 2, pp. 367–379, 2022.

[13] L. Zöllei, C. Jaimes, E. Saliba, P. E. Grant, and A. Yendiki, "Tracts constrained by underlying infant anatomy (traculina): An automated probabilistic tractography tool with anatomical priors for use in the newborn brain," *Neuroimage*, vol. 199, pp. 1–17, 2019.

[14] C. Maffei *et al.*, "Using diffusion mri data acquired with ultra-high gradient strength to improve tractography in routine-quality data," *NeuroImage*, vol. 245, p. 118706, 2021.

[15] G. Li, L. Wang, F. Shi, J. H. Gilmore, W. Lin, and D. Shen, "Construction of 4d high-definition cortical surface atlases of infants: Methods and applications," *Medical image analysis*, vol. 25, no. 1, pp. 22–36, 2015.

[16] K. H. Maier-Hein *et al.*, "The challenge of mapping the human connectome based on diffusion tractography," *Nature communications*, vol. 8, no. 1, pp. 1–13, 2017.

[17] A. Stocco *et al.*, "Analysis of the human connectome data supports the notion of a ?common model of cognition? for human and human-like intelligence across domains," *NeuroImage*, vol. 235, p. 118035, 2021.

[18] J. E. Laird, C. Lebiere, and P. S. Rosenbloom, "A standard model of the mind: Toward a common computational framework across artificial intelligence, cognitive science, neuroscience, and robotics," *Ai Magazine*, vol. 38, no. 4, pp. 13–26, 2017.

[19] D. Silver *et al.*, "Mastering the game of go with deep neural networks and tree search," *nature*, vol. 529, no. 7587, pp. 484–489, 2016.

[20] A. Graves *et al.*, "Hybrid computing using a neural network with dynamic external memory," *Nature*, vol. 538, no. 7626, pp. 471–476, 2016.

[21] P. R. Huttenlocher, "Morphometric study of human cerebral cortex development," *Neuropsychologia*, vol. 28, no. 6, pp. 517–527, 1990.